Imaging spectrometer technologies for advanced Earth remote sensing

J. B. Wellman, J. B. Breckinridge, P. Kupferman, R. P. Salazar, and K. B. Sigurdson

Jet Propulsion Laboratory, California Institute of Technology
4800 Oak Grove Drive, Pasadena, California 91109

Abstract

A major requirement of multispectral imaging systems for advanced Earth remote sensing is the provision for greater spectral resolution and more versatile spectral band selection. The imaging spectrometer instrument concept provides this versatility by the combination of pushbroom imaging and spectrally dispersing optics using area array detectors in the focal plane. The Shuttle Imaging Spectrometer concept achieves 10- and 20-meter ground instantaneous fields of view with 20-nanometer spectral resolution from Earth orbit. Onboard processing allows the selection of spectral bands during flight; this, in turn, permits the sensor parameters to be tailored to the experiment objectives. Recent advances in optical design, infrared detector arrays, and focal plane cooling indicate the feasibility of the instrument concept and support the practicability of a validation flight experiment for the Shuttle in the late 1980s.

Introduction

The broad range of user requirements for advanced land remote sensing is addressed in a companion paper.[1] From this study and others, the need for greater versatility in spectral coverage and spectral isolation within the 0.4- to 2.5-μm region emerges as a significant consideration in the design of future systems. The application of spectrometric techniques to pushbroom imaging[2,3,4] offers a method by which versatility in defining the individual spectral bands and the utilization of narrow spectral bands (high spectral resolution) can be realized.

Instrument concepts suitable for free-flying spacecraft, Shuttle-attached payloads, potential space platforms, and research aircraft have been studied. These concepts provide inherent registration of the many spectral channels in addition to the spectral versatility. Implementation of the imaging spectrometer concept requires technological advances in area array detectors for the visual and near-infrared (VNIR) and short-wavelength infrared (SWIR) spectral bands, in optical systems that provide imaging and spectral dispersion over the broad wavelength region, in focal plane cooling necessary for the achievement of acceptable signal-to-noise ratios, and in onboard electronics.

In the following presentation, we describe the Shuttle Imaging Spectrometer (SIS) as a prototypical example of the instrument system technology, discuss its performance capabilities, and review three supporting subsystem technologies: optics, focal-plane arrays, and focal-plane cooling.

Shuttle Imaging Spectrometer design

The formulation of observational requirements and needs for the SIS is based on the need for an instrument that would serve both as a research tool and a mechanism for verifying the technology. The constraints imposed on the SIS design include compatibility with the Shuttle, low cost in comparison to a free flyer (in consideration of the short duration missions), and a corresponding decrease in complexity. The intent was to develop a simple design that retained the major technological elements and fundamental performance capabilities, but dispensed with the operational requirements, most notably, swath width and complete global coverage.

From our analysis of the broad range of user's needs, a basic set of performance requirements was derived[4]. They are shown in Table 1. The spatial resolution of the system is specified by the ground instantaneous field of view (IFOV), an idealized measure defined by the cross-track geometric projection of a detector element or the along-track distance corresponding to the integration time (following the usual convention, these distances are designed to be equal). The radiometric precision is expressed as the noise equivalent change in reflectance (NEdR), which is defined as that change in ground reflectance that produces a change in detected signal equivalent to the instrument system noise level.

The dispersive approach, the key to the imaging spectrometer concept, uses area array detectors and accomplishes spectral separation by use of a spectrometer section added after the imaging optics. The concept is illustrated in Figure 1. Radiation from the scene is imaged upon a slit (oriented normal to the plane of the figure). The slit defines

Table 1. Shuttle Imaging Spectrometer Performance Requirements

Parameter	Value VNIR	SWIR
Ground IFOV, m	10	20
Spectral resolution, nm	20	20
Swath width, km	60	60
Radiometric precision, %	0.5	1.0

the system field stop and determines the footprint on the ground. Radiation passing through the slit is dispersed within a spectrometer and reimaged at the camera focal plane. Since the spectrometer is designed to maintain the spatial resolution present at the slit, the image at the spectrometer camera focal plane is a series of images of the line in object space, but displaced orthogonally in the spectral dimension as shown in Figure 2. This mapping of spatial and spectral information corresponds to a single line on the ground. The data to be transmitted by the instrument is read out from the focal plane in a short period of time. Within this time

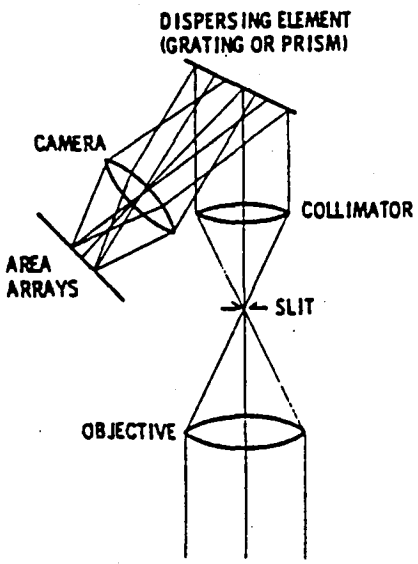

Figure 1. Imaging spectrometer optical concept

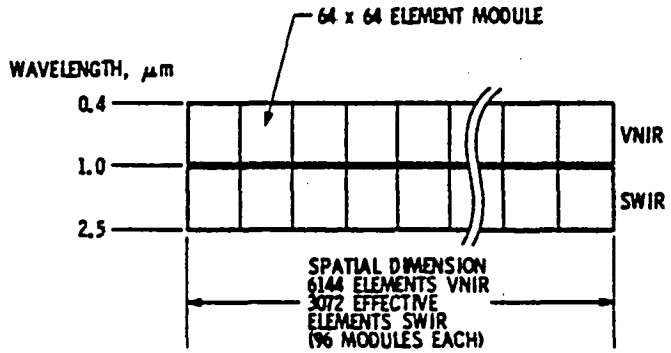

Figure 2. Shuttle imaging spectrometer focal surface arrangement

interval, the spacecraft motion moves the line image into the next position so that the imaging process can be repeated. The procedure is repeated continually to build up an image in the pushbroom manner.

With the information arranged in the focal plane as shown in Figure 2, considerable selectivity can be employed in the readout process. Individual spectral channels are confined to single rows within the detector; thus they can be extracted individually. Furthermore, the ability to sum adjacent rows in the readout structure of a charge-coupled device (CCD) permits broad spectral bands to be collected on the focal plane and read out as a single channel.

This dispersive approach offers several advantages over linear array approaches discussed elsewhere.[2,3] So long as the area arrays are oriented perpendicularly to the slit image, spectral registration is assured. The spectral dimension is typically one to two orders of magnitude smaller than the spatial dimension; thus the alignment problems are reduced by the corresponding factor when compared to the line array approaches. The dispersive approach provides higher spectral resolution and the opportunity to select a variety of spectral and spatial modes simply by varying the readout process. This degree of control can be exercised by ground command.

The significant disadvantage of the dispersive approach is complexity. The optical system is potentially larger and contains more elements. To preserve the desired radiometric precision at the narrower spectral channels, the aperture size must be increased, resulting in a weight penalty. The development of area array detectors is generally more difficult than that of line arrays. The supporting electronics must process more data at higher rates, which suggests increases in the power requirements. Although these penalties exist, the design efforts indicate that an instrument using the dispersive approach is technically and economically feasible, and that its performance advantages commend it for further development.

An iterative system design process was used to develop the instrument parameters that satisfy the stated performance requirements. The key detector parameters of element size

and noise performance were determined on the basis of experience with state-of-the-art detector arrays and feasibility studies for advanced array capability. The instrument aperture is sized to permit the achievement of the required NEdR. The resulting design characteristics are listed in Table 2.

Table 2. SIS Design Characteristics

Parameter	Value
Equivalent aperture diameter, cm	30
Telescope focal length, cm	120
Physical slit width, μm	40
Ground-projected slit width, m	10
Altitude, km	300
Swath width, km	61.44
Detector size (pixel), μm	40 × 40
Line time (for 10-m IFOV), ms	1.38
Encoding, bits/pixel	8
Raw data rate (VNIR), bits/s	2.27×10^9
(SWIR), bits/s	0.57×10^9
(Total), bits/s	2.84×10^9

SIS performance analysis

Major constraints on choice of system parameters arise because of limitations in the data rate, maximum size and speed of the optics, length and flatness of the focal plane, limitations in the butting of detector arrays, maximum detector array format and minimum pixel sizes, development of a linear prism disperser, and maximum integration times determined by the limitations imposed by pushbroom imaging. The design, developed in adherence to these constraints and summarized in Table 2, must satisfy the radiometric precision specification. The radiometric analysis is described in the following paragraphs.

We define NEdR to be that change in ground reflectance that produces a change in detected signal equivalent to the noise. The signal source is considered to be a perfectly diffusing target on Earth that reflects sunlight, which is attenuated by the atmosphere, towards the instrument. The NEdR is based on a reflectance scale of 100 percent, and the noise is a combination of signal and background shot noise and detector array readout noise.

The performance requirements in Table 1 call for differing spatial resolutions for the VNIR and SWIR. Since both arrays have the same format and physical size, the instantaneous footprints for the detectors are equal and designed to be 10 m. The 20-m IFOV for the SWIR channels is created by integrating for twice the basic line time and by summing the pixels in pairs during the readout process. These summations increase the signal-to-noise ratio because they occur prior to the readout amplifier. The data rate is reduced by a factor of four by these processes.

The working equations that incorporate these concepts are defined below. Equation (1) gives the signal per detector as a function of system parameters, Equation (2) the scene radiance at the instrument, Equation (3) the definition of noise, and Equation (4) the definition of NEdR.

$$S_\lambda = A\omega t\, \eta_\lambda\, T_\lambda\, N_\lambda\, d_\lambda \tag{1}$$

where

S_λ = signal in electrons for each band

A = effective primary area

ω = angular FOV subtended by the ground IFOV

t = integration time derived from given IFOV and spacecraft altitude

η_λ = detector quantum efficiency

T_λ = optical transmission of the system

N_λ = radiance of source at the aperture results from the solar irradiance attenuated by the atmosphere, isotropically scattered by a ground target of a given reflectance, and again attenuated by the atmosphere (Although not included here, the contribution to the signal from upwelling atmospheric radiance may be included in the design.)

$$N_\lambda = \frac{F_\lambda}{\pi} R_\lambda \cos i \ln\left[\left(1 + \frac{1}{\cos i}\right) \phi_\lambda\right] \tag{2}$$

where

πF_λ = solar irradiance outside the atmosphere

R_λ = ground reflectance

i = solar zenith angle

ϕ_λ = atmospheric transmission

$$N = \sqrt{S_\lambda + B + R^2} \tag{3}$$

where

N = rms noise in electrons

S_λ = signal in electrons

B = background signal in electrons. B is a function of background (instrumental) temperature and detector area, and is integrated over the entire detector spectral bandwidth. It is negligible for the 0.4- to 1.0-μm region

R = read noise in electrons (taken as 300 for the VNIR and 1000 for the SWIR)

$$\text{NEdR} = \frac{NR_\lambda}{S_\lambda} \tag{4}$$

where N, S_λ, and R_λ are defined above.

Using these relations, the NEdR as a function of wavelength is shown in Figure 3. The solid curve corresponds to the design spectral bandwidth of 20 nm. The dotted curve indicates the improvement in performance (smaller NEdR) gained by increasing the spectral bandwidth to 30 nm. The dashed curve shows the degraded performance (larger NEdR) achieved by decreasing the spectral bandwidth to 10 nm. The discontinuity at 1.0 μm results from the change from 10 m IFOV at shorter wavelengths to 20 m IFOV at longer wavelengths and the change in the detector noise figure from VNIR to SWIR values. The primary reason for the use of differing IFOVs for the VNIR and SWIR is to maintain the desired NEdR with a modest aperture dimension. Based on this analysis, the required NEdRs of 0.5 percent for the VNIR and 1.0 for the SWIR are met by all of the 20-nm spectral bands.

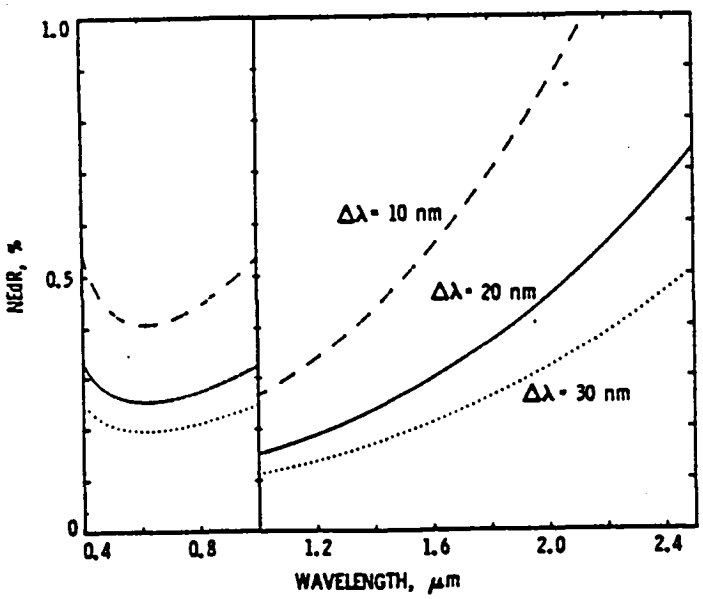

Figure 3. Radiometric performance characteristics of the SIS

This analysis assumes that the spectral dispersion is uniform across the spectral range. This condition does not generally hold for a prism spectrometer. A current design activity is to choose a combination of prism materials that will minimize the variation in spectral resolution over the 0.4- to 2.5-μm region.

Optical design

The most challenging optical design requirements are the field of view and spectral range over which the imaging performance is to be achieved. For the SIS requirements, a field of view of 8.6 deg must be provided over a spectral range from 0.4 to 2.5 μm. These requirements resulted in the design of an all-reflecting system with the single exception of the dispersing element. The wide spectral range, spanning three octaves in wavelength, combined with the low dispersion required and the high optical throughput goal, strongly argued for the use of a prism rather than a diffraction grating. Based on a careful tradeoff study, the Triple Reflecting Schmidt, Littrow Prism design[5] developed for the free-flyer instrument was selected. The design presented in this paper is a scaled version of the original design.

The optical design approach for the Shuttle Imaging Spectrometer, shown in Figure 4, consists of three reflecting Schmidt cameras, one for the foreoptics and two for the

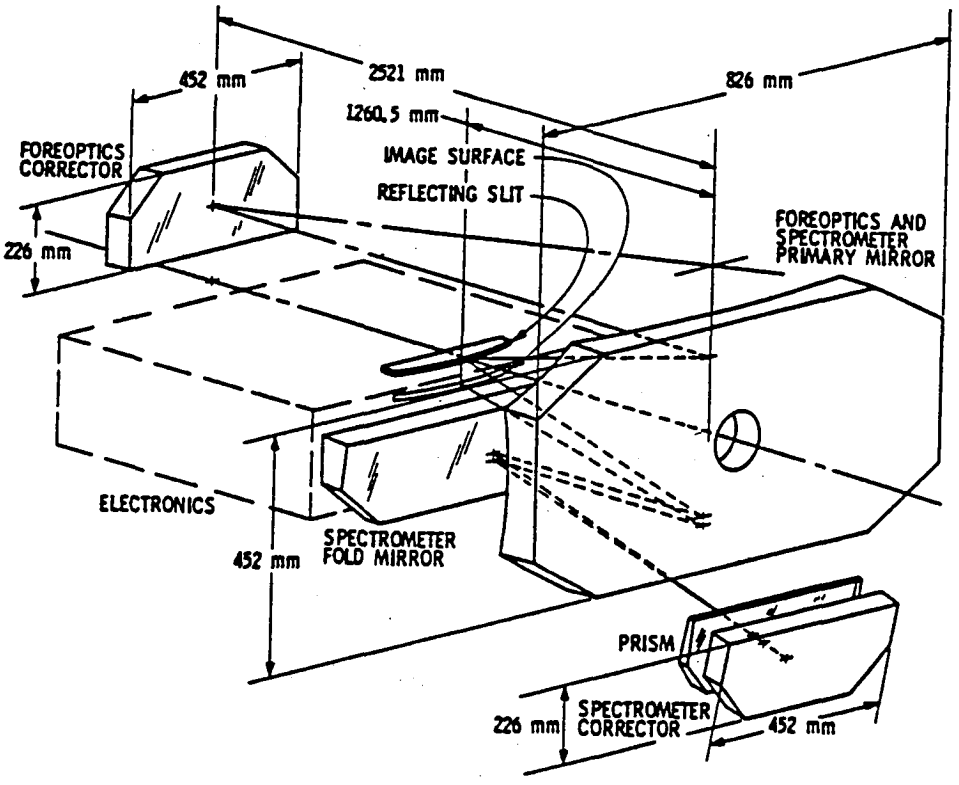

Figure 4. Shuttle imaging spectrometer optical configuration

spectrometer. The large primary mirror is shared by the three systems. Radiation enters the instrument through an aperture directly above the large primary mirror and strikes a D-shaped reflecting Schmidt corrector plate, located near the center of curvature of the spherical primary mirror. The corrector has the surface figure of a circular aspheric plate, but with the axis of symmetry passing below the bottom edge of the element. Radiation reflecting from the aperture corrector illuminates the upper portion of the primary mirror to produce an image at the primary focal surface, which is a sphere.

At the primary focal surface, a reflective slit defines the field stop and serves as the entrance slit for the spectrometer section. Serving also as a field flattener, the reflecting slit illuminates the lower portion of the primary, which now serves as the spectrometer collimator. A plane folding mirror directs the beam to the shallow prism. Radiation passing through the prism is reflected by another Schmidt corrector plate similar to the one used at the entrance to the foreoptics. The radiation is further dispersed as it makes its return pass through the prism, is folded back to the lower portion of the primary, which now serves as the spectrometer camera, and is imaged at the spectrometer focal surface. A small tilt in the spectrometer corrector displaces the spectrometer focal surface below the primary image focal surface, thereby leaving room for the detector arrays that populate the spectrometer focal surface.

The use of the fold mirror provides a large unobscured volume immediately behind the focal plane; this volume facilitates detector cooling and the convenient location of the supporting electronics.

The optics were ray-traced for design, tolerances, and focal-plane metrology using the ACCOS V interactive computer-aided design program. The focal surface lies on a spherical surface of 2.5-m radius. It is curved slightly with a deviation from the chord of 0.63 mm at the short wavelength end. This slight curvature can be accommodated by adjusting the locations of the detector arrays in the alignment of the focal plane. Designs that reduce this curvature are currently being evaluated.

The image quality of the system can be inferred from the isometric views of the point spread functions shown in Figure 5. The boundaries of each plot define the 40-μm-square pixel size. The spatial coordinate is indicated by Y; the spectral by X. The polarization of the instrument is less than one percent and is probably limited by the residual polarization present in thin-film mirror coatings.

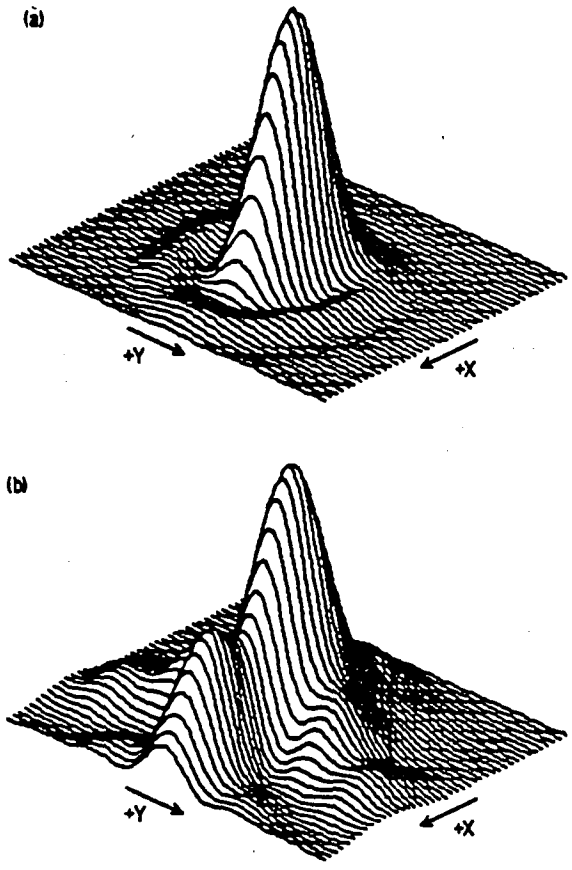

Figure 5. Optical point spread functions: (a) on-axis; (b) full-field

Focal-plane implementation

The most significant challenge in the implementation of the SIS is the short-wavelength infrared focal plane. Detector arrays of the performance and format needed do not presently exist, although a major development program is underway. Based on an assessment of the several IR technologies being developed, the hybrid approach using mercury-cadmium-telluride photodiodes with a 2.5-μm cutoff wavelength has been selected for this design. The arrays consist of two parts: a photodiode array made of the appropriate IR detecting material, and a CCD multiplexer, which collects the photogenerated charge and transfers it to an on-chip amplifier for readout. The two elements are interconnected with an array of indium column bonds, one for each pixel. This technology has been demonstrated, but not for the specific wavelength performance characteristics and format needed by SIS.

Development of mercury-cadmium-telluride detector arrays for imaging spectrometer applications has been underway at the Rockwell International Science Center.[6] Three 32 × 32 element hybrid arrays with 68-μm-square pixels and a 4.5-μm cutoff wavelength have been fabricated and tested prior to delivery to the Jet Propulsion Laboratory for characterization and use in the Airborne Imaging Spectrometer.[7] Indium column interconnect yields of 100% have been achieved. A significant improvement in pixel-to-pixel uniformity of response can be seen in the detectivity histogram of Figure 6. Arrays with a 2.5-μm cutoff wavelength will be developed and evaluated in the next phase of the effort.

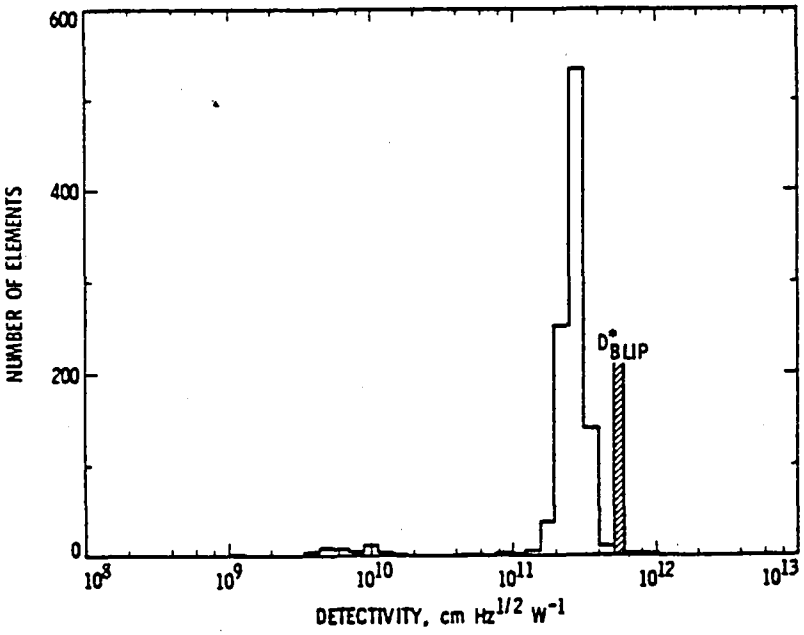

Figure 6. Detectivity (D^*) histogram for 32 × 32 HgCdTe hybrid detector array at 77 K and high background (5 × 10^{15} photons $cm^{-2}s^{-1}$).

Forecasts of the technology suggested that a development goal of a 54-by-64 element format with a 2.5-μm cutoff wavelength could be met within the next few years, and that flight quality arrays could be produced with sufficient yield to support a space flight program in the latter half of the decade. Accordingly, the SIS design was developed around this building block.

The visual and near-infrared detectors, covering the 0.4- to 1.0-μm spectral range, chosen were silicon CCD imagers. By comparison to the SWIR arrays, the silicon CCDs do not represent a major technology challenge. For the purposes of this design, the detectors were defined as having the same format and dimensions as the SWIR arrays. The focal plane configuration shown in Figure 2 is a mosaic of both types of array. The arrays are mosaicked or butted on two sides to create a focal plane with 6144 elements in the spatial dimensions and 64 elements in each of the SWIR and VNIR spectral dimensions. A total of 96 arrays in each wavelength group is needed to populate the focal plane.

An alternative approach for detection in the SWIR wavelength range is the relatively mature indium-antimonide photodiode technology (developed by Cincinnati Electronics Corp.) coupled with a novel multiplexed readout technique.[8,9,10] A 128-element linear array with good uniformity and more than adequate detectivity for the application has been demonstrated. A 512-element linear array is under development using the same technique. Use of multiple linear arrays in place of area array detectors offers the possibility of a near-term demonstration of the imaging spectrometer technique prior to commitment to the full-scale development of the SIS.

Focal-plane cooling

To perform properly, the infrared detector arrays must be cooled to temperatures on the order of 130 K. (The alternative focal-plane technology using indium-antimonide detectors requires temperatures below 90 K.) Studies conducted in conjunction with the free-flyer design indicate that the required temperatures could be attained using an advanced, passive, radiative cooler.[11] A Shuttle mission poses different problems, most notably the inability of a radiator to view cold space. The alternative that appears to offer the best potential for meeting temperature and heat-load requirements reliability for long Shuttle or platform missions is the adsorption refrigerator.[12] In this system, high-pressure gas is supplied to a Joule-Thomson refrigerator by an adsorption compressor. In the compressor, the working gas is adsorbed by a solid at low temperatures and pressures. Low-quality heat, either waste or solar, is utilized to desorb the gas. The resulting high-pressure gas is then passed through a Joule-Thomson valve, which cools the gas. The heat load from the detectors is transferred to the gas, which flows back to the compressor/adsorber (exchanging heat with the incoming gas along the way) where it is readsorbed upon cooling of the compressor. This results in a closed system that has only self-operating check valves for moving parts. It is thus expected to be inherently reliable for long-life applications.

A conceptual diagram of this system is shown in Figure 7. The two compressors shown would be used alternately to insure a continuous supply of cold gas to the refrigeration chamber. A heat source and sink must be alternately connected and disconnected from the compressor for the system to operate. The two heating sources envisioned are solar heating, using electrically actuated louvers to cycle the heat supply, or waste electrical heat, using thermal switches. Both approaches would have few moving parts and would be inherently reliable.

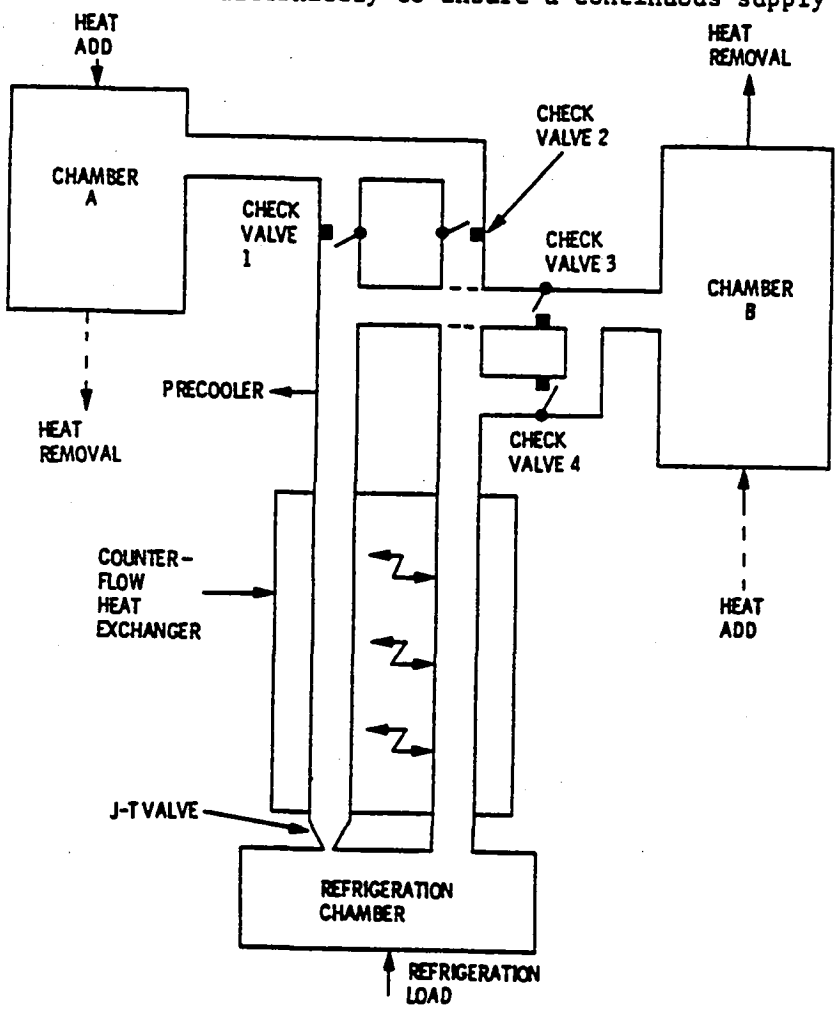

Figure 7. Adsorption refrigeration block diagram

The adsorption refrigerator offers the strong advantages of reliability, a lower power requirement, and insensitivity to spacecraft configuration and orbit over a broad range of operating temperatures. This device is applicable to large space platforms, whereas radiators are unlikely to be usable because of geometry problems. It can also be used in an evolutionary manner on short Shuttle flights by replacing the adsorption chambers with a mechanical compressor or an expendable supply of high-pressure gas.

Conclusions

The SIS instrument design is responsive to the future requirements of both research- and applications-oriented users. As an experimental tool, the SIS provides a great deal of versatility with which the spectral domain can be explored at high resolution. The

technology elements on which the SIS concept depends are being pursued both within this program and on related efforts.

The optical design presented here and several variations under study are capable of satisfying the performance requirements and can be implemented with standard optical fabrication processes. The reflecting slit poses some unusual fabrication challenges, which will be addressed in future work. Further exploration of linearizing the spectral dispersion and correcting the focal-plane curvature are expected to simplify the focal-plane mosaic implementation.

The required SWIR performance levels have been achieved with two materials – mercury cadmium telluride and indium antimonide – and suitable multiplexing techniques have been demonstrated. Challenges remain in optimizing the performance for the 1.0- to 2.5-μm spectral region and in developing structures suitable for mosaicking into large focal-plane arrays.

Cooling methodologies for both Shuttle and free-flyer instrument concepts have been examined. Both the adsorption refrigerator and radiative coolers are capable of providing focal-plane operation at temperatures as low as 80 K; thus the detector choices need not be severely restricted by temperature constraints. The development of a breadboard adsorption refrigerator sized for the SIS application is planned.

We conclude that the performance requirements identified in this paper can be met and that continued progress in the supporting technologies will permit a space-flight verification of the imaging spectrometer approach in the latter half of the 1980s.

Acknowledgements

The authors wish to acknowledge the efforts of the Imaging Spectrometer Design Team at JPL, the contributions of Professors R. R. Shannon and R. V. Shack and their students at the University of Arizona in optical design, and the detector array development efforts led by Dr. J. Rode of Rockwell International Science Center and B. Fehler of Cincinnati Electronics Corporation.

The research described in this publication was carried out by the Jet Propulsion Laboratory, California Institute of Technology, under contract with the National Aeronautics and Space Administration.

References

1. Vane, G., Billingsley, F. C., and Dunne, J. A., "Observational Parameters for Remote Sensing in the Next Decade," Paper No. 345-06, in Proceedings of the Society of Photo-Optical Instrumentation Engineers, May 4-7, 1982.

2. Wellman, J. B., "Multispectral Mapper: Imaging Spectroscopy as Applied to the Mapping of Earth Resources," Paper No. 268-19, in Proceedings of the Society of Photo-Optical Instrumentation Engineers, D. D. Norris, ed., 268, February 10-11, 1981.

3. Wellman, J. B., "Technologies for the Multispectral Mapping of Earth Resources," in Proceedings of the Fifteenth International Symposium on Remote Sensing of Environment, Vol. I, Environmental Research Institute of Michigan, Ann Arbor, Michigan, May 11-15, 1981.

4. Wellman, J. B., Breckinridge, J. B., Kupferman, P. N., and Salazar, R., "Imaging Spectrometer: An Advanced Multispectral Imaging Concept," 1982 International Geoscience and Remote Sensing Symposium, Munich, Federal Republic of Germany, June 1-4, 1982.

5. Breckinridge, J., Page, N., and Shannon, R., Applied Optics, 1982 (in preparation).

6. Vural, K., Acceptance Test Report, Contract No. 955949, Rockwell International Science Center, Thousand Oaks, California, 1982.

7. Wellman, J. B., and Goetz, A. F. H., "Experiments in Infrared Multispectral Mapping of Earth Resources," Paper No. 80-1930, AIAA Sensor Systems for the 80's Conference, Colorado Springs, Co., December 2-4, 1980.

8. Bailey, G. C., "Design and Test of the Near Infrared Mapping Spectrometer (NIMS) Focal Plane for the Galileo Jupiter Orbiter Mission," in Proceedings of the Society of Photo-Optical Instrumentation Engineers, 197, August 29-30, 1979.

9. Bailey, G. C., "An Integrating 128 Element Linear Imager for the 1 to 5 μm Region," in Proceedings of the Society of Photo-Optical Instrumentation Engineers, 311, 1981.

10. Bailey, G. C., "An Integrating 128 Element InSb Array: Recent Results," Paper No. 345-23, in Proceedings of the SPIE, May 4-7, 1982.

11. Bard, S., Stein, J., Petrick, S., "Advanced Radiative Cooler with Angled Shields," Paper No. 81-1100, AIAA 16th Thermophysics Conference, Palo Alto, Calif., June 23-25, 1981.

12. Chan, C. K., "Cryogenic Refrigeration Using a Low Temperature Heat Source," Cryogenics, 391-399, July 1981.